Available online at www.sciencedirect.com
SCIENCE DIRECT®
Journal of Solid State Chemistry 178 (2005) 1595–1600
JOURNAL OF SOLID STATE CHEMISTRY
www.elsevier.com/locate/jssc

Synchrotron diffraction studies of TiC/FeTi cermets obtained by SHS

L. Contreras[a], X. Turrillas[b], M.J. Mas-Guindal[a], G.B.M. Vaughan[c], Å. Kvick[c], M.A. Rodríguez[a,*]

[a]*Instituto de Cerámica y Vidrio, CSIC, 28049 Madrid, Spain*
[b]*Eduardo Torroja Institute for Construction Sciences, CSIC, 28033 Madrid, Spain*
[c]*European Synchrotron Radiation Facility, 38043 Grenoble, France*

Received 7 December 2004; received in revised form 7 March 2005; accepted 8 March 2005

Abstract

TiC/FeTi composites have been obtained in situ by Self-propagating High-temperature Synthesis (SHS) of an intimate mixture of compacted powders of elemental carbon, titanium and iron. The reaction has been followed in real time by X-ray diffraction at the ESRF. The mechanism of the reaction is discussed in terms of the formation of a liquid phase corresponding to the eutectic of the Fe/Ti system prior to the TiC synthesis. Temperatures of reaction have been estimated by correlating thermal expansion coefficients with diffraction peaks shifts. The microstructures obtained by this method, suitable for cutting tools and wear resistant applications, are presented.

Keywords: SHS; Combustion synthesis; Synchrotron; X-ray diffraction; Intermetallics; Cermet

1. Introduction

Self-propagating High-temperature Synthesis (SHS), also known as combustion synthesis is an inexpensive and straightforward method of obtaining single and multiphase materials by exploiting the self-sustaining capability of highly exothermic reactions, once initiated. Usually, the reaction is triggered by some external heat source—either electrical or chemical—and then proceeds as a reaction front with linear velocities that range from 1 to 100 mm/s depending on the products and the process conditions. This has been extensively used to produce different kinds of compounds varying from hard refractory carbides, nitrides and borides to oxides, chalcogenides or even intermetallics [1]. In some cases the formation of one compound can release enough heat to favor the reaction of materials that otherwise would not react by themselves in a self-sustaining mode. Therefore, this approach allows the preparation of composites in a single stage synthesis. Contrarily, a traditional melting and mixing method would require a more complex and multi-step process and large quantities of energy.

Metal matrices embedded with hard ceramic powders (cermets) have been widely used as precursor powders for thermal spray coatings, cutting tools, wear resistant parts, in armoured vehicles and jet engine fuel pump rotors among others [2]. The aim of our work has been to prove the feasibility of obtaining TiC/FeTi intermetallic cermets by SHS. For a review on the various synthesis routes of TiC reinforced ferrous-based composites see for example Ref. [3].

The understanding of the synthesis mechanisms for these systems that can reach extreme temperatures and occur at very high speeds have far-reaching consequences, more precisely in improving and optimising their industrial production and design.

The European Synchrotron Radiation Facility in Grenoble, France, delivers a high flux of X-rays that

*Corresponding author. Fax: +34 91 7355843
E-mail address: mar@icv.csic.es (M.A. Rodríguez).

0022-4596/$ - see front matter © 2005 Elsevier Inc. All rights reserved.
doi:10.1016/j.jssc.2005.03.011

can be used in many ways to study processes in which intense, monochromatic, highly collimated beams are needed. The Materials Science Beamline ID11 offers the possibility to carry out diffraction experiments that, due to its high flux and fast detection capabilities, can detect intermediate phases formed in extremely rapid reactions, as is the case of SHS processes.

Its excellent performance has allowed us to monitor phase changes with time resolutions of 65 ms per diffraction pattern, which is enough to detect very short lifespan intermediates or even phase transitions occurring before melting or on cooling.

Also, precise determination of the diffraction peaks displacement, due to the heating and consequent expansion during the reaction, of some selected diffraction peaks, has allowed us to estimate the temperatures achieved during the process and relate them to the observed transitions.

Finally, SEM images provided information about the microstructures obtained in order to confirm some aspects of the proposed mechanism.

2. Experimental

2.1. Starting materials and sample preparation

The following starting materials have been used: (a) Pure Ti metal > 98% (William Rowland Ltd., UK) with particle size $d_{50} = 84\,\mu m$, and specific surface $Ss = 0.03\,m^2/g$. (b) Graphite powder 99.6% (Sofacel, Spain) with particle size $d_{50} = 1.7\,\mu m$, $Ss = 2.7\,m^2/g$. (c) Atomised iron powder > 99.0% pure (William Roland Ltd., UK) with particle size < 500 μm.

The starting materials were mixed in molar proportions, according to the stoichiometric reaction: C/Fe/2Ti.

The initial powders were thoroughly mixed in a porcelain mortar and axially pressed in a 20 mm diameter stainless steel die. A pressure of 30 MPa was applied to obtain 2 mm thickness cylindrical pellets with an apparent density corresponding to ≈55% of the theoretical value.

2.2. Scanning electron microscopy

SEM photographs were performed with a Zeiss DSM-950 microscope. The specimens were embedded in an epoxy resin under vacuum to facilitate their polishing on a lapping disk with diamond paste to a degree of 1 μm smoothness. The polished surface was cleaned with absolute ethanol, dried and finally gold coated by sputtering.

2.3. Synchrotron X-ray diffraction

The ESRF ID-11 Materials Science beamline was used. It can deliver an intense X-ray flux in the energy range 5–100 keV employing a vacuum undulator of 138 poles with a period of 23 mm and a minimum magnetic gap of 5 mm. For these experiments the gap was set to 8 mm to get a radiation with a local maximum of energy distribution around 47 keV. A wavelength of 0.26102 Å with an energy band path of $\Delta E/E = 10^{-4}$ was selected with a double-crystal Si (111) monochromator; the first crystal is liquid nitrogen cooled and the second bent to provide a sagittally focused beam. A further focusing was applied with an X-ray lens developed by Snigirev et al. [4] and an order of magnitude increase of the number of photons reaching the sample was achieved. Two couples of slits delimited the irradiated area on the specimen to $50 \times 20\,\mu m^2$.

With these settings a satisfactory compromise between spatial resolution, penetration of sample and counting statistics of the diffracted signal, within the geometric restrictions of the setup, was attained.

The detailed experimental setup for the data acquisition was described in Ref. [5]. Here, a briefer description is exposed. A graphite sample-holder with three degrees of freedom along x, y and z, held the compacted pellets. It was assured that the center of the sample was hit by the X-ray beam. A Frelon CCD camera collected a 15° 2Θ diffraction cone in transmission mode. This camera characterised by its low noise and its small readout time—lower than 0.1 s—has a resolution of 2048×2048 pixels. These features coupled to the implemented optics and scintillators, let getting an effective pixel size between 0.4 and 40 μm [6].

The experiments were carried out in air. To ignite the pellet, a narrow trail, 15 mm long, of titanium powder was placed at its bottom. This way, when a current was fed through a V-shaped tungsten wire in contact with an extreme of the titanium trail, the reaction was initiated and the reaction front travelled from the bottom to the top of the pellet. To overcome the computer memory limitation, which only allowed the acquisition of a 600 diffraction patterns series, the electrical signal was sent approximately 5 s before launching the data acquisition.

Although 35 ms were enough to get a diffraction pattern, 30 ms took the transmission of data, hence adding a dead time which increased the effective time resolution to 65 ms. The control software Spec [7] under Linux implemented in a workstation was used for the data acquisition.

2.4. Data processing

The diffraction rings of the images were integrated with computer scripts linked to Fit2D [8] and developed at ID11. Upon integration, standard files containing information of angle, intensity and its associated error were created, which subsequently were read with scripts written in IDL [9]. The selected diffraction peaks were fitted to Gaussian curves using the algorithms

implemented in IDL. For the general plotting of graphs, Origin 7.0 [10] was used and for the two-dimensional contour maps, Transform [11].

3. Results and discussion

To get a good spatial resolution a small diffracting volume was selected. The drawback was loosing some statistical representativeness. Undoubtedly, the chances of striking a single crystallite are much higher and that is what actually happened: even the integrated diffraction patterns showed sudden intensity burst as a consequence. Nevertheless the resolution was excellent, for example the position of Ti (004) reflection presented a FWHM of $0.09 \pm 0.003^\circ$ 2Θ, the peaks position could be determined with good precision and its peak shape could be fitted satisfactorily to Gaussian functions. Because of this erratic behavior of intensities, any attempt of doing Rietveld analysis was unfruitful, even applying orientation corrections. Unfortunately, this texturing effect is more pronounced in metals and alloys prepared by SHS due to the orientation created by the unidirectional reaction front. This front is perpendicular to the pressing axis as well as to the incident beam, nevertheless, no study has been carried out to clarify the influence of the orientation of the compaction axis. Despite all these limitations, it was possible to select some reflections to follow the reaction pathway and to calculate temperatures from their displacements. However, the analysis to calculate the temperatures via peak shifts on heating and cooling during the entire reaction could not be made. Some regions, particularly at higher temperatures, did not present exploitable diffraction patterns for this purpose.

The onset of the reacting synthesis produces many phase transformations, which permit the simultaneous presence of high- and low-temperature forms of the metals. On the other hand, the existence of interactions between species which appear and disappear, during a period of about 5 s, does not leave any peak that could be singled out to perform temperature calculations by the method that will be described in some extension in the next paragraph.

3.1. Temperature profiles

The reaction was studied taking advantage of the new detector capabilities which allow broader angular range capture with a better time resolution due to its improved counting statistics. The entire reaction to be studied can be summarized as follows:

$$C + Fe + 2Ti \rightarrow TiC + FeTi. \quad (1)$$

The whole process, that takes place in about 40 s, is presented in Fig. 1 as a contour plot derived from individual diffraction patterns sequentially represented as a pseudo-three-dimensional map.

One of the major problems of studying these processes is to get accurate temperature profiles as the SHS reaction progresses. In a recent work [12] where synchrotron radiation was used in conjunction with infrared cameras, the temperature profiles show a time resolution matching the one obtained by diffraction. However, this method only measures the temperature at the surface and since the cooling is faster at the surface the measurements do not correctly follow the

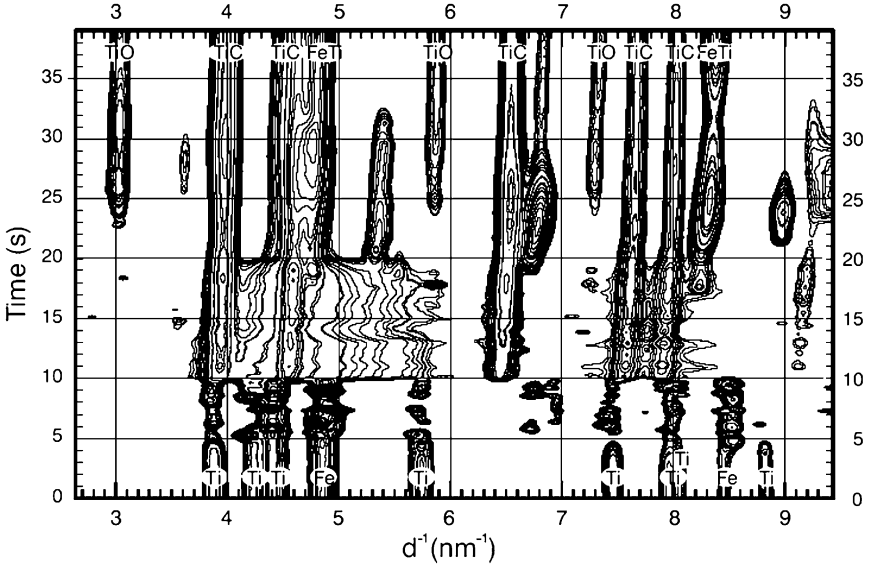

Fig. 1. General contour map of the reaction. It is a projection from a three-dimensional map obtained by positioning the whole sequence of diffraction patterns. The initial and final phases are highlighted.

temperature combustion in the bulk. A second problem could be added: the spot probed by the infrared camera may not coincide either in position or in size with the one used to obtain the diffraction pattern. Therefore, the pyrometer readings may not arise from the actual diffracting volume when is reached by the reaction front.

To overcome these difficulties we have adopted a different strategy. The diffraction data have been used to deduce the temperature. Indeed, the peak positions are defined with sufficient accuracy to be correlated with temperature by using available thermal expansion data. The final XRD patterns obtained at room temperature acted as reference to calibrate the 2Θ zero shift. The main associated error is related to Bragg's Law and would be responsible for an error of ≈ 100 K, being conservative. The Ti (004) reflection was chosen to deduce the temperature evolution—being isolated and relatively high in angle—while the α-Ti to β-Ti transition was chosen as a reference in temperatures for the heating process. A second zone was estimated following the β-Ti (110) reflection. Some points of the heating curve could be obtained following the evolution of the FeTi (110) reflection, though the appearance and disappearance of this species prior to the reaction to form TiC, did not allow having a complete curve of this zone. The cooling curve is based on the shift of TiC (111) reflection, selected with similar criteria, and the last diffraction pattern was the reference for temperatures in this zone. Thermal expansion coefficients for Ti and TiC were taken from Ref. [13]. As it was previously mentioned, a few seconds before the reaction occurred, no single peak could be chosen that could be useful for temperature calculations. The experimental curve of the process, shown in Fig. 2, is compatible with a cooling model that takes into account both radiative and convective effects, except in some areas where deviations are due to exothermic reactions which take place during the cooling. Such is the case of the plateau in the vicinity of 1000 °C. The use of this approximation has been previously described with more detail in Ref. [14].

3.2. Diffraction analysis

Taking into account the temperature profiles and inspection of the X-ray diffractograms, the process, that takes place in about forty seconds as a whole, can be divided into the following steps that are related with the Fe/Ti phase diagram [15]. See Fig. 3.

(a) *Ignition*. At time 0 s, the initial products, Fe and Ti can be seen but graphite is barely visible due to its low scattering factor and small crystallites size—very finely divided powder.
(b) *Heating and re-crystallization*. During the first 5 s diffraction peaks shift to lower angles and some of

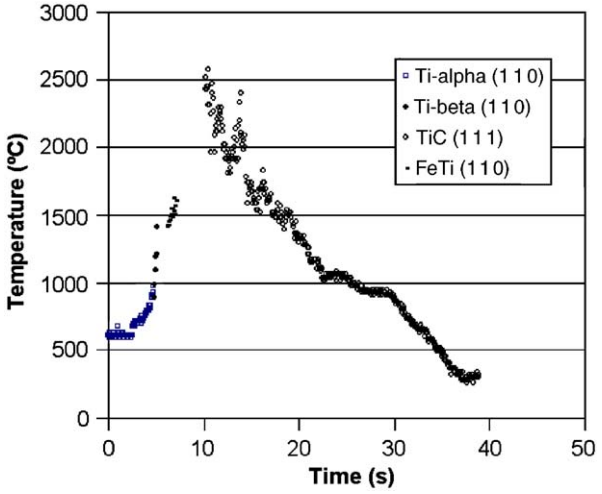

Fig. 2. Temperature profile along the reaction. Bold hexagons represent the temperatures obtained from diffraction peaks of α-Ti (100), open squares from β-Ti (110), open diamonds from FeTi (110) and bold squares from TiC (111).

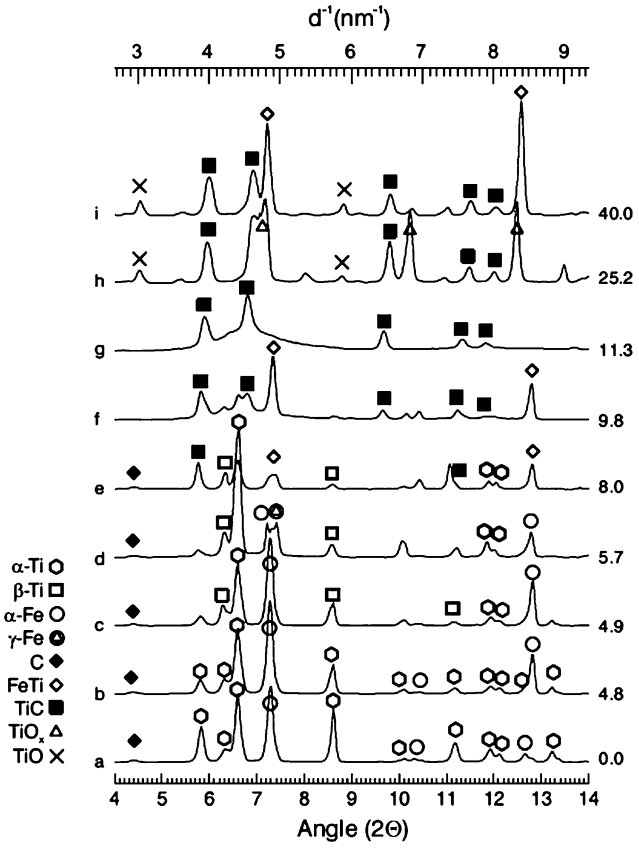

Fig. 3. Some diffraction patterns chosen on the critical stages of the reaction are shown to explain the mechanism. On the right side, time in seconds, (a) initial products. (b) Re-crystallisation. (c) Phase transformation of Ti. (d) Phase transformation of Fe. (e) Appearance of liquid. (f) Appearance of TiC and consumption of C. (g) Everything molten except TiC. (h) Intermediate species. (i) Final products.

them, abnormally, increase their intensities due to texturing effects.

(c) *Phase changes of the metals*. First β-Ti appears coexisting with the low temperature α phase, corresponding with an estimated temperature of about 893 °C that fits properly with the phase diagram of the system.

(d) $\alpha \rightarrow \gamma$ iron transformation. Both species can be observed and persist until 8.0 s.

(e) Appearance of liquid phase, with diminishing intensities of all diffracted peaks, that according to the phase diagram is formed by the eutectic of the FeTi/Ti system, and then FeTi precipitation. During this period it is possible to calculate the temperature of the reaction for a few seconds following FeTi (110) reflection. Temperature continues to increase due to the exothermic character of FeTi formation, which in the end produces re-melting of the intermetallic with the disappearance of the corresponding peaks. Also, TiC seems to appear at this stage.

(f) Upon the appearance of liquids, the diffusion of carbon into the droplets speeds up and initiates the reaction to form TiC, the most favored compound among the possible ones, according to thermodynamic calculations.

(g) Once carbon dissolves and precipitates as TiC, a sudden boost in temperature is observed and any existing solid except titanium carbide melts. This event happens about 2 s after first liquids appear. For approximately 7 s the metals remain molten, although occasionally some peaks appear for one or two diffractograms, probably due to precipitation and instantaneous re-dissolution. Temperature estimation of this part of the process, yielding a maximum of about 2515 °C is in very good agreement with other authors' data [16]. After this, as cooling progresses, some fluctuations can be observed in the curve above 2000 °C. This phenomenon has been observed by other authors [16] in the combustion of the Fe–Ti–C system, in which a thermocouple was used to measure temperatures. An explanation could be the different velocities of diffusion, and hence of re-precipitation, of carbon in droplets of Ti or Fe [17]. Our data cannot confirm nor deny this supposition.

(h) Upon further cooling, solid species begin to precipitate affecting the cooling rate. The heat released by this crystallization provokes a plateau in the 20–30 s region of approx. 1100 °C in the time/temperature curve that fits well with the Fe–Ti/Ti eutectic in the phase diagram. One of the species has been identified as stoichiometric FeTi but it has not been possible to assign with certainty the other diffraction peaks. They might be attributed to some less common titanium oxides.

(i) Finally, this intermediate species disappear yielding as final products TiC and a b.c.c. solid solution of Fe/Ti with FeTi structure, probably due to a deviation from the theoretical stoichiometry. Other species in the Fe/Ti system, such as Fe_2Ti, have not been detected. Some small peaks can be assigned to partially oxidised metals: i.e. TiO, the most probable compound expected on thermodynamic grounds, in the presence of small quantities of oxygen.

3.3. Morphological studies

SEM observations (Fig. 4) show the microstructures sought, obtained by combustion synthesis. Small (1–2 μm) rounded particles of TiC embedded in a ferrotitanium alloy matrix with good interfacial adhesion have been attained. Some porosities are found but fully dense material cannot be obtained unless external pressure is applied during the SHS reaction. EDS semi-quantitative analysis confirmed the ferrotitanium nature of the matrix even though small variations in the Fe/Ti composition were perceived. This microstructure is compatible with a dissolution–precipitation synthesis.

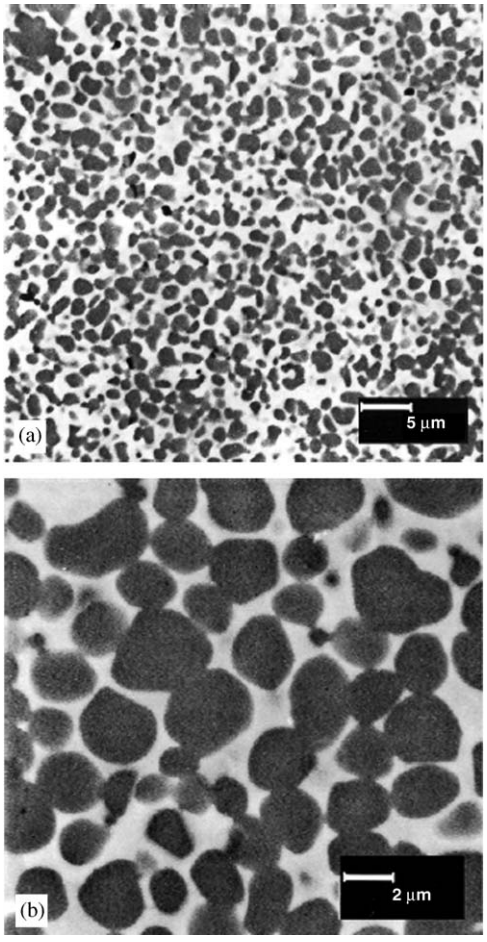

Fig. 4. SEM micrographs of the obtained materials with two magnifications.

4. Conclusions

Self-propagating high temperature synthesis has proved to be a straightforward way to obtain very homogeneous intermetallic matrix composites with hard ceramic TiC as reinforcement, taking advantage of the high exothermic nature of TiC formation.

Synchrotron X-ray diffraction is an advantageous tool for the study of very fast reactions due to the new capabilities of detection and data handling at the ESRF, opening the possibility of studying complex mechanisms of reactions which involve phase changes, short existence phases and molten species.

A temperature profile assessment can be achieved, due to the good quality of the diffraction patterns. Indeed, the peak shifts due to known thermal expansion coefficients of some of the phases involved in the reaction can be related to the temperature. Therefore, it is feasible to outline a quite precise temperature profile.

The use of those profiles in conjunction with phase diffraction analysis facilitates the interpretation of reaction mechanisms.

Carbon, titanium and iron react in a self-sustained mode, yielding a ferrotitanium matrix, with a FeTi b.c.c. structure, TiC-reinforced composite with the appropriate characteristics to be used in hard and wear resistant utensils.

Acknowledgments

We thank the ESRF for beamtime granted through experiment CH-1235. This work has been supported by the Spanish Science and Technology Agency (CICYT) under project No. MAT 2000-0941.

References

[1] Z.A. Munir, U. Anselmi-Tamburini, Mater. Sci. Rep. 3 (1989) 277.
[2] R.M. Hathaway, P.K. Rohatgi, N. Sobczak, J. Sobczak, Proceedings of the International Conference on High Temperature Capillarity, 1997.
[3] K. Das, T.K. Bandyopadhyay, S. Das, J. Mater. Sci. 37 (2002) 3881.
[4] A. Snigirev, V. Kohn, I. Snigireva, B. Lengeler, Nature 384 (1997) 49.
[5] J.C. Labiche, et al., ESRF Newslett. 25 (1996) 41.
[6] C. Curfs, I.G. Cano, G.B.M. Vaughan, X. Turrillas, Å. Kvick, M.A. Rodríguez, J. Eur. Ceram. Soc. 22 (2002) 1039.
[7] SPEC, Certified Scientific Software, Cambridge, MA.
[8] A. Hammersley, S.O. Svensson, A. Thompson, Nucl. Instrum. Methods A 346 (1994) 312.
[9] Research Systems Inc. (Kodak Company), Sterling, VA, USA. Program IDL Version 5.2 (2002). www.rsinc.com
[10] OriginLab Corporation, Northampton, MA, USA. Program Origin Version 7.0 (1999). www.OriginLab.com
[11] Research Systems Inc. (Kodak Company), Sterling, VA, USA. Program IDL Version 5.2 (1998). www.rsinc.com
[12] D. Vrel, N. Girodon-Boulandet, S. Paris, J.F. Mazué, E. Couqueberg, M. Gailhanou, D. Thiaudière, E. Gaffet, F. Bernard, Rev. Sci. Instrum. 73 (2000) 422.
[13] D.R. Lide (Ed.), Handbook of Chemistry and Physics, CRC Press, New York, 1998.
[14] L. Contreras, X. Turrillas, G.B.M. Vaughan, Å. Kvick, M.A. Rodríguez, Acta Mater. 52 (2004) 4783.
[15] J.L. Murray, Bull. Alloy Phase Diagrams (1981) 320.
[16] A. Saidi, A. Chrysantou, J.V. Wood, J.L.F. Kellie, Ceram. Int. 23 (1997) 185.
[17] Q. Fan, H. Chai, Zh. Jin, J. Mater. Sci. 36 (2001) 5559.